THE ASTROPHYSICAL JOURNAL, 612:L93–L96, 2004 September 10

CANDIDATES OF $z \simeq 5.5$–7 GALAXIES IN THE *HUBBLE SPACE TELESCOPE* ULTRA DEEP FIELD

HAOJING YAN[1] AND ROGIER A. WINDHORST[2]

Received 2004 March 17; accepted 2004 July 23; published 2004 August 6

ABSTRACT

We report results from our $z \simeq 5.5$–7 galaxy search in the *Hubble Space Telescope* Ultra Deep Field (UDF). Using the 400 orbit of Advanced Camera for Surveys data, we found 108 plausible $5.5 \leq z \leq 6.5$ (or $z \simeq 6$ for short) candidates to $m_{\rm AB}(z_{850}) = 30.0$ mag. The contamination to the sample, due to either image artifacts or known types of astronomical objects, is likely negligible. The inferred surface densities of $z \simeq 6$ galaxies are consistent with our earlier predictions from $m_{\rm AB}(z_{850}) = 26.5$ to 28.5 mag. After correcting for detection incompleteness, the counts of $z \simeq 6$ candidates to $m_{\rm AB}(z_{850}) = 29.2$ mag suggest that the faint-end slope of the galaxy luminosity function (LF) at this redshift is likely between $\alpha = -1.8$ and -1.9, which is sufficient to account for the entire Lyman photon budget necessary to complete the reionization of the universe at $z \simeq 6$. We also searched for $z \simeq 6.5$–7 candidates using the UDF Near-Infrared Camera and Multi-Object Spectrometer data and have found four candidates to a magnitude of $J_{110} = 27.2$. However, the infrared colors of three candidates cannot be easily explained by galaxies in this redshift range. We tentatively derive an upper limit to the cumulative surface density of galaxies at $z \simeq 7$ of 0.36 arcmin^{-2} to a magnitude of $J_{110} = 26.6$, which suggests a noticeable drop in the LF amplitude from $z \simeq 6$ to $z \simeq 7$.

Subject headings: cosmology: observations — early universe — galaxies: evolution — galaxies: high-redshift — galaxies: luminosity function, mass function

Online material: machine-readable table

1. INTRODUCTION

Using the Advanced Camera for Surveys (ACS), a public, ultradeep survey has been carried out by the *Hubble Space Telescope* (*HST*). This Ultra Deep Field (UDF; PI: S. Beckwith) campaign observed a single ACS Wide Field Camera (WFC) field within the Chandra Deep Field–South in four broad bands covering 0.4 to nearly 1.0 μm. To enhance the value of these ACS data, the Camera 3 (NIC3) of the Near-Infrared Camera and Multi-Object Spectrometer (NICMOS) has observed the central portion of this field in the F110W (J_{110}) and F160W (H_{160}) filters (PI: R. Thompson). With a total exposure of 400 orbits in the ACS and 144 orbits in the NICMOS, the UDF will remain the deepest optical/IR survey field in the coming 7 years. Here we discuss the $z \simeq 5.5$–7 candidates found in this field. We adopt the following cosmological parameters: $\Omega_M = 0.27$, $\Omega_\Lambda = 0.73$, and $H_0 = 71$ km s^{-1} Mpc^{-1}. All magnitudes are in the AB system.

2. DATA AND SELECTION OF $z \simeq 6$ AND $z \simeq 7$ CANDIDATES

The total UDF ACS/WFC exposure times are 37.5, 37.6, 96.4, and 96.3 hr in the F435W (B_{435}), F606W (V_{606}), F775W (i_{775}), and F850LP (z_{850}) filters, respectively. The final drizzle-combined stacks have a pixel scale of 0.″03 and cover an effective area of 10.34 arcmin^2 after trimming off the lower signal-to-noise ratio (S/N) edges. We performed matched-aperture photometry independently using SExtractor (Bertin & Arnouts 1996) in double-input mode with the z_{850} stack as the detection image. We used a 5 × 5 Gaussian convolving kernel with an FWHM of 3 pixels, and we required that a real detection have a minimum of 5 connected pixels 1.5 σ above background. The NIC3 UDF program observed a 3 × 3 grid that covers the center of the UDF, giving an effective coverage of 5.76 arcmin^2 with an average exposure time of 5.97 hr in both the J_{110} and H_{160} filters. The final drizzle-combined stacks have a pixel scale of 0.″09. We used the photometric catalog that comes with the data release, which was generated based on the detections in the co-added $J_{110} + H_{160}$ stack using SExtractor. The "MAG_AUTO" option was used in both cases.

We selected $z \simeq 6$ candidates as i_{775} dropouts in the UDF ACS images. Instead of aiming at $z \geq 6.0$ and using the color criterion of $(i_{775} - z_{850}) \geq 2.0$ mag as in our previous work (Yan et al. 2003), we here target at $5.5 \leq z \leq 6.5$ and adopt $(i_{775} - z_{850}) \geq 1.3$ mag as the first criterion. In total, 108 objects were selected by using this color criterion alone. These objects were visually examined in all four bands to ensure that there was no obvious reason (e.g., image defects) to exclude them from the candidate list. The second criterion is that a valid candidate should not be detected in B_{435} and V_{606}; i.e., it should either have a reported magnitude fainter than 29.5 mag or have its estimated photometric error larger than 0.54 mag (S/N < 2). All of the 108 candidates satisfy this criterion. The coordinates and the photometric properties of all the 108 candidates are listed in Table 1.[3] These objects seem to be strongly clustered; e.g., we identified six multiple systems whose members are within 1″ (or <5.8 comoving kpc) from each other. The significant fraction of multiple systems might indicate that merging was rather common at $z \simeq 6$.

Fifty-two of the 108 candidates are within the NIC3 mosaic, among which 12 objects (all at $z_{850} < 27.8$ mag) have NIC3 counterparts. Actually, nine of these 12 objects are in four multiple systems, and the coarser pixel resolution of the NIC3 images cannot resolve their individual members and thus identify them as single sources. The $z_{850}J_{110}H_{160}$ colors of these 12 objects (nine sources in four multiple systems, and three isolated sources) are shown in Figure 1. The z_{850} magnitudes of

[1] *Spitzer* Science Center, California Institute of Technology, MS 100-22, Pasadena, CA 91125; yhj@ipac.caltech.edu.

[2] Department of Physics and Astronomy, Arizona State University, Box 871504, Tempe, AZ 85287-1504.

[3] The brighter half of these objects [to $m_{\rm AB}(z_{850}) < 28.5$ mag] was also independently reported by Bunker et al. (2004).

TABLE 1

PHOTOMETRIC PROPERTIES OF THE $z \simeq 6$ CANDIDATES[a]

ID[b]	R.A., Decl. (J2000)[c]	S/G[d]	FWHM[e]	i_{775}	z_{850}	$i-z$	J_{110}	H_{160}
1a	3 32 40.01, −27 48 15.01	0.04	5.0	26.88 ± 0.03	25.25 ± 0.01	1.62	25.47 ± 0.02	25.41 ± 0.02
1b	3 32 40.04, −27 48 14.54	0.00	12.6	29.03 ± 0.18	27.41 ± 0.07	1.62		
2a	3 32 36.47, −27 46 41.45	0.02	9.6	29.00 ± 0.16	26.49 ± 0.03	2.51	26.60 ± 0.04	25.92 ± 0.03
2b	3 32 36.49, −27 46 41.38	0.02	6.1	29.58 ± 0.22	27.76 ± 0.07	1.82		
3	3 32 38.28, −27 46 17.22	0.06	6.0	29.77 ± 0.29	26.68 ± 0.03	3.09	26.83 ± 0.04	26.73 ± 0.04
4	3 32 34.55, −27 47 55.97	0.02	6.6	28.62 ± 0.10	26.93 ± 0.04	1.70	26.76 ± 0.03	26.60 ± 0.03
5a	3 32 34.29, −27 47 52.80	0.00	14.3	29.07 ± 0.21	26.97 ± 0.05	2.10	26.56 ± 0.03	26.70 ± 0.04
5b	3 32 34.28, −27 47 52.26	0.00	14.9	28.98 ± 0.19	27.17 ± 0.06	1.80		
5c	3 32 34.31, −27 47 53.56	0.00	15.3	29.42 ± 0.22	27.76 ± 0.08	1.66		
6	3 32 33.43, −27 47 44.88	0.00	7.5	29.31 ± 0.18	27.23 ± 0.05	2.09	27.22 ± 0.03	27.28 ± 0.04
7a	3 32 37.46, −27 46 32.81	0.00	13.0	32.49 ± 4.00	27.50 ± 0.07	4.99	26.61 ± 0.02	26.26 ± 0.02
7b	3 32 37.48, −27 46 32.45	0.00	11.7	29.70 ± 0.30	27.78 ± 0.09	1.92		

[a] Photometric properties of the 108 $z \simeq 6$ candidates discovered in the UDF. The first 12 objects are the candidates that have been identified in the UDF NICMOS images. Table 1 is published in its entirety in the electronic edition of the *Astrophysical Journal*. A portion is shown here for guidance regarding its form and content.

[b] There are six multiple systems among these candidates, four of which are within the NICMOS UDF area. The members of these systems have their ID in boldface. Note that object 1a is a known galaxy at $z = 5.83$.

[c] Units of right ascension are hours, minutes, and seconds, and units of declination are degrees, arcminutes, and arcseconds.

[d] S/G is the star/galaxy separation code, with 0 for the most extended sources and 1 for the most compact sources.

[e] The FWHM (in units of pixels) is derived by assuming a Gaussian core.

the multiple systems are derived by adding the fluxes of their individual members. The known $z = 5.83$ galaxy (Dickinson et al. 2004; Stanway et al. 2004) is among these four multiple systems (ID 1a in Table 1).

Candidates of $z \simeq 7$ objects were selected as z_{850}-band dropouts. As the J_{110} band heavily overlaps with the z_{850} band, the $(z_{850} - J_{110})$ color at $z > 6.5$ does not change as dramatically as the $(i_{775} - z_{850})$ color does at $z \simeq 6$. We adopted the criteria as $(z_{850} - J_{110}) > 0.8$ mag and $(J_{110} - H_{160}) > -0.1$ mag, with no detection in ACS B_{435}, V_{606}, and i_{775} bands. This search resulted in one z_{850} source and three z_{850} dropouts, all of which were visually inspected and deemed reliable. The coordinates and the photometric properties of the three z_{850} dropouts are listed in Table 2. The one z_{850} source turns out to be the multiple system 7a/7b in Table 1 (and also qualifies as being $z \simeq 6$) and thus is not listed again.

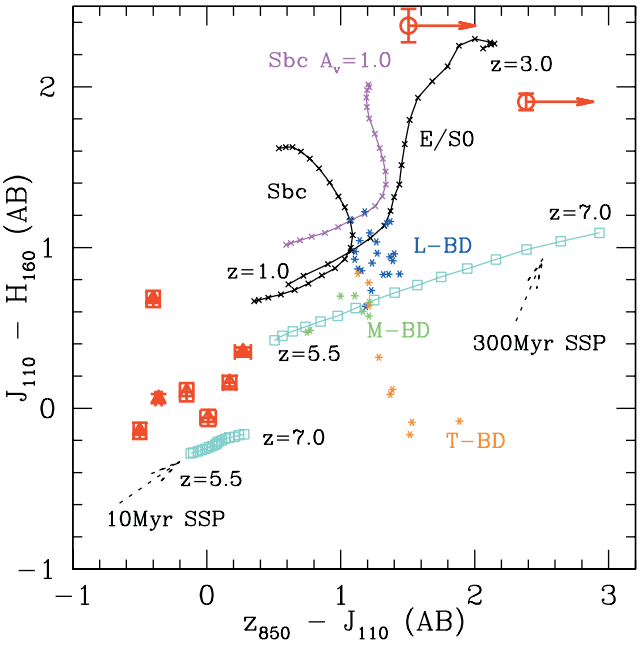

FIG. 1.—The $z \simeq 6$ candidates detected by NIC3 shown as red triangles with error bars (the four multiple systems are shown as filled triangles). These objects are well separated from the locations of possible interlopers such as low-z E/S0 galaxies or brown dwarfs. Their colors are consistent with star-forming galaxies at $z \simeq 6$, if the variations in SED (such as ages and different star formation history) and the systematic errors in photometry are considered. The open circles with error bars and $(z_{850} - J_{110})$ color upper limits represent the first two of the three z_{850} dropouts in Table 2, whose z_{850} limits are more securely determined. However, their colors suggested that they are not likely at $z \simeq 7$ but are more likely lower redshift early-type galaxies.

3. DISCUSSION OF THE $z \simeq 6$ CANDIDATE SAMPLE

3.1. *Consistency of the $z \simeq 6$ Interpretation*

It is known that brown dwarfs can mimic the broadband colors of a $z \simeq 6$ galaxy because of their strong molecular absorption bands. The 4000 Å break in elliptical galaxies at $z \simeq 1.0$–1.5 can also mimic the Lyman break at $z \simeq 6$ (e.g., Yan et al. 2003). Lower z late-type galaxies, even those significantly reddened by dust, generally are not a significant interloper, because their 4000 Å breaks are not as strong as those in the early-type galaxies.

The contamination due to brown dwarfs is insignificant in our case, as only four of our 108 candidates have a SExtractor star/galaxy separation flag larger than 0.90. This flag is 0 for extended sources and 1 for point sources. The colors of typical M-, L-, and T-type brown dwarfs (BDs; e.g., Kirkpatrick et al. 1999) are shown in Figure 1. None of the $z \simeq 6$ candidates with NIC3 measurements have IR colors close to the loci of brown dwarfs. The contamination due to elliptical galaxies at $z \simeq 1.0$–1.5 is likely also small. While the major color criterion is $(i_{775} - z_{850}) > 1.3$ mag, most of the candidates have $(i_{775} - z_{850}) > 1.5$ mag (90 out of 108), and thus the chance for a low-z elliptical galaxy to be selected as candidate is greatly reduced, since the latter usually have $(i_{775} - z_{850}) \leq 1.3$ mag. Further evidence comes from the candidates also detected in NIC3 images. Figure 1 shows the "color track" of a typical E/S0 galaxy in $z_{850} J_{110} H_{160}$ space, together with the tracks of an Sbc galaxy with and without dust reddening (all templates are from Coleman et al. 1980, and the extinction law is from Calzetti et al. 2000). None of the NIC3 detected $z \simeq 6$ candidates have colors close to these low-z tracks. On the other hand, the colors of our candidates are consistent with being $z \simeq 6$, if we consider the systematic photometric errors due to the aperture mismatching between the ACS and the NIC3 photometry and,

TABLE 2

PHOTOMETRIC PROPERTIES OF THE THREE z_{850} DROPOUTS FOUND IN THE UDF NICMOS FIELD[a]

ID	R.A., Decl. (J2000)[b]	z_{850}(limit)[c]	J_{110}	H_{160}
1	3 32 38.74, −27 48 39.97	28.97	26.58 ± 0.05	24.68 ± 0.01
2	3 32 42.88, −27 48 09.52	28.52	27.01 ± 0.10	24.63 ± 0.02
3	3 32 42.56, −27 46 56.69	28.45	27.30 ± 0.06	26.11 ± 0.02

[a] The very red IR colors of these three z_{850} dropouts suggest that they are more likely lower redshift early-type galaxies. The only probable $z \simeq 7$ candidate left in our sample (not shown here) is the object pair 7a/7b in Table 1, which could be at the border of the $z \simeq 6$ bin and the $z \simeq 7$ bin.

[b] Units of right ascension are hours, minutes, and seconds, and units of declination are degrees, arcminutes, and arcseconds.

[c] These magnitude limits are obtained by adding the flux within an aperture of 0.″54 radius, which is not necessarily the size of the apertures that are used for J_{110} and H_{160} photometry.

more importantly, the variation in the spectral energy distribution (SED) of $z \simeq 6$ galaxies. While a detailed stellar population synthesis approach is beyond the scope of this Letter, we point out that most of the candidates in Figure 1 can be well explained by the models of Bruzual & Charlot (2003). For simplicity, Figure 1 shows the color tracks of the simple stellar population (SSP) models with ages of 10 and 300 Myr, which bracket most of the $z \simeq 6$ candidates.

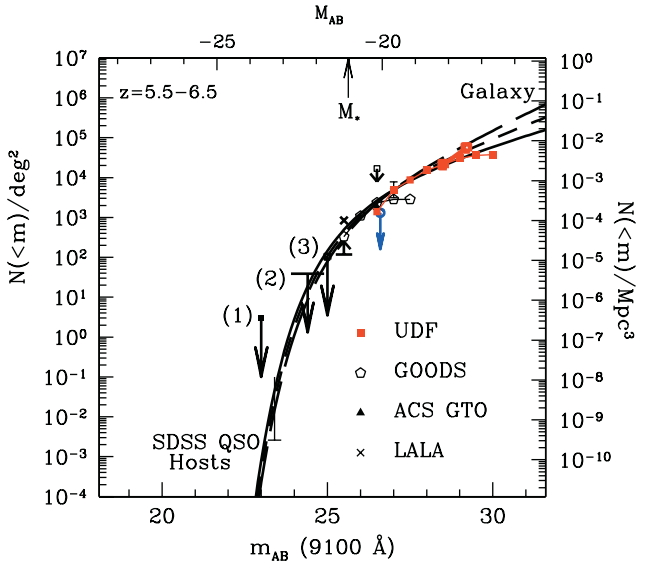

FIG. 2.—The cumulative surface densities of $z \simeq 6$ galaxies at different brightness levels inferred from the $z \simeq 6$ candidates sample in this Letter agree very well with our earlier predictions, which were extrapolated from the galaxy LF measured at $z \simeq 3$ (Yan et al. 2002). The normalization of the LF estimate at $z \simeq 6$ is fixed by the cumulative number density of $z \simeq 6$ galaxies in the HDF-N to a limit of AB = 27.0 mag. This prediction is consistent with the available observations (see YW04) and is reproduced here for three different LF faint-end slopes: $\alpha = -1.6$ (*solid line*), -1.8 (*short -dashed line*), and -2.0 (*long -dashed line*). Without correction for incompleteness at faint fluxes, our UDF result suggests a LF faint-end slope of $\alpha = -1.6$ or slightly flatter. However, after applying a correction to incompleteness in the flux range $z_{850} = 28.5$–29.2 mag, the inferred cumulative number density to a magnitude of 29.2 could be a factor of 3.51 higher (indicated by the open red box) and is consistent with a steeper faint-end slope of $\alpha = -1.8$ to -1.9. Given that the incompleteness correction cannot be zero, a faint-end slope steeper than -1.6 is plausible. Based on the discussion of YW04, this clearly suggests that "normal" galaxies can account for the entire reionizing photon budget at $z \simeq 6$. The amplitude of the LF at $z \simeq 7$ could be significantly lower, which is indicated by our derived upper limit (*the blue downward arrow*).

3.2. *Photometric Contamination and Correction for Incompleteness*

When the search is pushed to very faint levels, contamination due to noise spikes could become severe. To assess the effect due to spurious detections, we performed the "negative source" check as described by Dickinson et al. (2004). The UDF ACS mosaics were inverted, and SExtractor was run on these inverted images using the same parameter settings as in § 2. We find only 10 "negative objects" that have S/N ≥ 3, and *none* of them satisfy our color selection criterion of $(i_{775} - z_{850}) \geq 1.3$ mag. This is not surprising because the UDF ACS mosaics were created by stacking a very large number of dithered images (the z_{850} band mosaic has 288 ditherings), so that the image artifacts are minimal. Therefore, we conclude that spurious detection has a negligible impact on our candidate sample.

Another effect that should be considered is sample incompleteness, which starts to be significant at $z_{850} > 28.5$ mag. We note that the z_{850}-band count histogram peaks at 28.5 mag (S/N ≃ 10) and drops to 50% of this peak value at 29.2 mag (S/N ≃ 7). For our purpose below, it is sufficient to discuss only the incompleteness of the candidates in the intermediate brightness range of $28.5 < z_{850} < 29.2$ mag. We estimated the incompleteness as follows. For each of the 28 candidates in this regime, a 11 × 11 pixel image "stamp" centering on the object was copied from the z_{850}-band mosaic. Each stamp was then added to the z_{850}-band mosaic at ~550 randomly distributed positions. Source detection was performed on these simulated images to recover the artificially added objects. We find that the median recovering rate is 28.5%, corresponding to an incompleteness correction factor of 3.51.

3.3. *Luminosity Function of Galaxies at $z \simeq 6$ and Reionization*

In Yan et al. (2002), we made a prediction of the luminosity function (LF) of galaxies at $z \simeq 6$ based on the measured galaxy LF at $z \simeq 3$. As summarized in Yan & Windhorst (2004, hereafter YW04), this LF estimate agrees well with all available observations (e.g., Rhoads et al. 2003; Yan et al. 2003; Stanway et al. 2003; Bouwens et al. 2003; Dickinson et al. 2004). Based on this LF, it was also suggested in YW04 that "normal" galaxies can account for the entire ionizing photon budget necessary to finish the reionization of the universe by $z \simeq 6$, as long as the faint-end slope of the LF is sufficiently steep. This LF, with slopes of $\alpha = -1.6$, -1.8, and -2.0, is reproduced in Figure 2. YW04 predicted that the UDF data would reveal 50–80 $z \simeq 6$ objects to a magnitude of $z_{850} = 28.4$. Among

the 108 candidates reported here, 55 objects are brighter than this level, and this agrees with our earlier prediction.

As discussed in YW04, if the nominal clumping factor value ($C = 30$ at $z = 5$) is adopted, normal galaxies can account for the entire reionizing photon budget at $z \simeq 6$ as long as the faint-end slope of the LF at this redshift is somewhat steeper than -1.6 and the normalization of the LF is close to what we estimated. If the faint-end slope is shallower than -1.6, galaxies cannot meet the reionization requirement unless the clumping factor is significantly lower, the LF normalization is much higher, or the Lyman photon escaping fraction is larger. Since all evidence indicates that the LF normalization is about right, the important issue is the faint-end slope of the $z \simeq 6$ LF. No other data set is better than the UDF $z \simeq 6$ candidate sample for this purpose. The cumulative number densities inferred from our sample, without incompleteness correction, are plotted as filled red boxes in Figure 2. Again, these numbers agree well with our LF prediction to a magnitude of 28.5, where the candidate selection does not suffer from severe incompleteness. However, as Figure 2 also shows, we have to measure the counts to significantly fainter than 28.5 mag in order to constrain the possible range of faint-end slopes. While our data points beyond 28.5 mag seem to suggest a faint-end slope of $\alpha = -1.6$ or even shallower, this is rather biased by the incompleteness at the faint levels. If we apply the correction as mentioned in § 3.2, a steeper slope is indicated. The open red box in Figure 2 shows the corrected cumulative surface density to a magnitude of 29.2, if a factor of 3.51 is applied to the density of the intermediate brightness group ($z_{850} = 28.5$–29.2 mag), which suggests a faint-end slope between $\alpha = -1.8$ and -1.9. For comparison, if the incompleteness correction were only a factor of 2 for the intermediate brightness group—contrary to what our simulation indicates—a faint-end slope of -1.7 would still be required. Therefore, we conclude that the major sources of the reionization at $z \simeq 6$ are indeed normal galaxies with dwarflike luminosities. It is interesting to note that Stiavelli et al. (2004) have also reached the similar conclusion, although from a different approach, that regular galaxies at $z \simeq 6$ are sufficient for reionization.

4. CONSTRAINT TO THE LF AT $z \simeq 7$

While our $z \simeq 7$ candidate sample has four objects, further investigation shows that a $z \simeq 7$ interpretation is not straightforward. First of all, the three z_{850} dropouts have $(J_{110} - H_{160}) > 1$ mag, which makes them also J_{110} dropouts. As a $z \simeq 7$ object should have similar fluxes in both J_{110} and H_{160} bands, they are unlikely to be at this redshift. We also explored a large variety of dust-reddened young galaxy templates and found that none of them could have such a large break across the J_{110} band. We note that the first two objects in Table 2 are similar to the *J*-band dropout object (but slightly brighter) found by Dickinson et al. (2000) in the Hubble Deep Field–North (HDF-N), whose nature is yet unclear. Second, the remaining candidate in the $z \simeq 7$ sample is likely at the border of the $z \simeq 6$ bin and the $z \simeq 7$ bin, as this candidate is actually the multiple system 7a/7b in the $z \simeq 6$ sample. Therefore, whether this system should be counted as $z \simeq 6$ or $z \simeq 7$ is very uncertain at this stage.

Nevertheless, we can still derive a useful *upper* limit of the cumulative surface density of $z \simeq 7$ galaxies based on objects 7a/7b, assuming that both members are at $z > 6.5$. This limit is 0.36 arcmin^{-2} to a magnitude of $J_{110} = 26.6$. While there are a number of reported Lyα emitters at $z > 6.5$, a direct comparison against these results is difficult because these Lyα emitters either are gravitationally lensed by foreground clusters (Hu et al. 2002; Kneib et al. 2004) or do not have continuum magnitudes available (Kodaira et al. 2003; Rhoads et al. 2004). However, none of these results seem to be in conflict with our derived upper limit.

Assuming no evolution from $z \simeq 6$ to 7, our LF predicts that the cumulative surface density of $z \simeq 7$ galaxies to a magnitude of 26.6 is 0.51 arcmin^{-2}, which is somewhat higher than the observed upper limit. Thus, our data suggest a noticeable drop of the LF amplitude over 0.16 Gyr from $z \simeq 6$ to 7, which we tentatively identified with the onset of galaxy formation and the onset of the first regular initial mass function of Population II stars, the low-mass end of which we still see in galaxy halos today, and the high-mass end of which finished reionization at $z \simeq 6$, when those hot stars resided in dwarf galaxies at $z \simeq 7$–6.

5. SUMMARY

We searched for $z \geq 5.5$–7 galaxy candidates in the UDF, using the UDF WFC and NIC3 data. We have found 108 $z \simeq 6$ candidates to a limit of $z_{850} = 30.0$ mag, which is consistent with the prediction in YW04. The cumulative surface densities after the correction of incompleteness suggest a slope of $\alpha = -1.8$ to -1.9, which means galaxies can account for the reionizing photon budget at $z \simeq 6$. We also searched for $z \simeq 7$ galaxy candidates but only found one such object whose redshift might be at the lower end of the redshift range under question. The search also resulted in three z_{850} dropouts, whose colors shown that they are not likely at $z > 7$. The paucity of $z \simeq 7$ candidates suggests that the LF amplitude drops significantly beyond $z \simeq 6$, which can be identified with the dawn of galaxy formation.

The authors thank the referee for very helpful comments. We acknowledge the support from the NASA grant HST-GO-09780. H. Y. acknowledges the support provided by NASA through contract 1224666 issued by the JPL, Caltech under NASA contract 1407.

REFERENCES

Bertin, E., & Arnouts, S. 1996, A&AS, 117, 393
Bouwens, R. J., et al. 2003, ApJ, 595, 589
Bruzual A., G., & Charlot, S. 1993, ApJ, 405, 538
Bunker, A. J., Stanway, E. R., Ellis, R. S., & McMahon, R. G. 2004, MNRAS, submitted (astro-ph/0403223)
Calzetti, D., et al. 2000, ApJ, 533, 682
Coleman, G. D., Wu, C.-C., & Weedman, D. W. 1980, ApJS, 43, 393
Dickinson, M., et al. 2000, ApJ, 531, 624
———. 2004, ApJ, 600, L99
Hu, E. M., Cowie, L. L., McMahon, R. J., Capak, P., Iwamuro, F., Kneib, J.-P., Maihara, T., & Motohara, K. 2002, ApJ, 568, L75
Kirkpatrick, J. D., et al. 1999, ApJ, 519, 802
Kneib, J.-P., Ellis, R. S., Santoas, M. R., & Richard, J. 2004, ApJ, 607, 697
Kodaira, K., et al. 2003, PASJ, 55, L17
Rhoads, J. E., et al. 2003, AJ, 125, 1006
———. 2004, ApJ, 611, 59
Stanway, E. R., Bunker, A. J., & McMahon, R. G. 2003, MNRAS, 342, 439
Stanway, E. R., Bunker, A. J., McMahon, R. G., Ellis, R. S., Treu, T., & McCarthy, P. J. 2004, ApJ, 607, 704
Stiavelli, M., Fall, S. M., & Panagia, N. 2004, ApJ, 610, L1
Yan, H., & Windhorst, R. 2004, ApJ, 600, L1 (YW04)
Yan, H., Windhorst, R., & Cohen, S. 2003, ApJ, 585, L93
Yan, H., Windhorst, R. A., Odewahn, S. C., Cohen, S. H., Röttgering, H. J. A., & William, C. K. 2002, ApJ, 580, 725